CSIRO PUBLISHING

Australian Journal of Physics

Volume 50, 1997

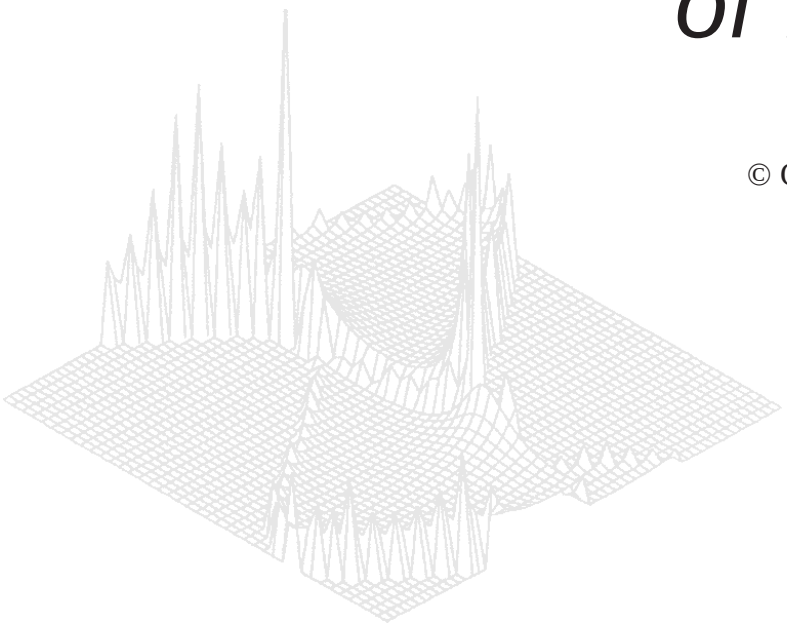

A journal for the publication of
original research in all branches of physics

www.publish.csiro.au/journals/ajp

All enquiries and manuscripts should be directed to
Australian Journal of Physics
CSIRO PUBLISHING
PO Box 1139 (150 Oxford St)
Collingwood Telephone: 61 3 9662 7626
Vic. 3066 Facsimile: 61 3 9662 7611
Australia Email: peter.robertson@publish.csiro.au

Published by **CSIRO** PUBLISHING
for CSIRO Australia and
the Australian Academy of Science

Aust. J. Phys., 1997, **50**, 553–75

Boundary Effects in the Townsend–Huxley Experiment*

J. P. England[A] *and H. R. Skullerud*[B]

[A] Atomic and Molecular Physics Laboratory,
Research School of Physical Sciences and Engineering,
Australian National University, Canberra, ACT 2600, Australia.
[B] Department of Physics, Norwegian University of Science and Technology,
N-7034 Trondheim, Norway.

Abstract

The Townsend–Huxley transverse diffusion experiment has been modelled using kinetic theory, with the aim of explaining the successes and shortcomings of some current ratio formulae that are based on hydrodynamic theory. These are shown to be essentially identical in form, apart from the estimated magnitudes of the boundary layer corrections to the second and fourth transverse position moments of the current density. The main reason for the shortcomings is shown to be the inability of hydrodynamic theory to describe the relaxation of the input electron energy distribution towards the steady state free space form. As a byproduct of the studies, exact eigensolutions have been found for the associated 'infinite slab' problem, using the constant collision frequency model with the two-term approximation.

1. Introduction

The experimental study of the behaviour of electron swarms in gases and electrostatic fields has been one of the most important sources of accurate information about low energy electron–molecule collision processes. Typically, transport coefficients such as drift velocities, diffusion coefficients and reaction rates have first been measured as functions of the electric field to density ratio E/n_0 and the gas temperature, and kinetic theory has subsequently been used to relate the behaviour of these 'macroscopic quantities' with the variation of collision cross sections with the collision energy. The transport coefficients are quantities describing the evolution of the swarm in the absence of physical boundaries, and the experiments should therefore ideally be performed in a 'free space environment'. The real experimental arrangements do, however, invariably have material boundaries, and this to some extent influences the experimental results and complicates their interpretation.

One may try to minimise the influence of the boundaries by using apparatus dimensions large compared with the expected extent of the boundary layers. At high E/n_0 values, this is however often not possible, because of the onset of electrical breakdown. Alternatively, one may use a variable length apparatus, and attempt to subtract out the end effects by differencing, or measure at a series of densities n_0 and attempt an extrapolation of the results to conditions $n_0 \to \infty$. A more convenient way of approach would be to apply some theoretically or empirically based correction formula, to allow precise values for the transport coefficients to be obtained from single measurements.

* Dedicated to Professor Robert W. Crompton on the occasion of his seventieth birthday.

10.1071/PH96072 0004-9506/97/030553$10.00

In the present paper, we present a theoretical study of boundary effects in the Townsend–Huxley transverse diffusion experiment, which is designed to measure accurately the ratio D_T/μ between the transverse diffusion coefficient D_T and the mobility μ. The aim of the study has essentially been to explain why a semi-empirical current ratio formula derived by Huxley (see Huxley and Crompton 1974) has been more successful in the analysis of experimental data than a formula derived by Lowke (1971) from a careful solution of the anisotropic diffusion equation. Parts of the work have been presented briefly at two Swarm Seminars (England and Skullerud 1991, 1993).

We will first discuss the experiment and the current ratio formulae, and show how the latter for practical purposes can all be written in the same form but with different numerical coefficients, and thus be easily compared. We then show how to formulate a suitable kinetic theory description of the experiment, and further present two complementary approaches to the solution of the kinetic equations, one applicable in the weak field regime and the other in the strong field regime. Only elastic 'quasi-Lorentz gas models' will be considered.

The work draws heavily on the vast literature on the associated one-dimensional slab problem, for the quasi-Lorentz gas problem (e.g. Lowke *et al.* 1977; Braglia and Lowke 1979; Robson 1981; Braglia 1982), and also for the pure Lorentz gas problem (e.g. Davison and Sykes 1957; Williams 1971; Cole *et al.* 1984), the steady state Townsend experiment (e.g. Sugawara *et al.* 1992; Robson 1995), and the, in many ways rather similar, quasi-Rayleigh gas problem (e.g. Burscha and Titulaer 1982; Beals and Protopopescu 1983; Naqvi *et al.* 1984). We have abstained from trying to trace the origin of all ideas used, and apologise to those who may find references lacking.

2. Idealised Townsend–Huxley Experiment

(2a) Experimental Conditions

The experimental setup is shown schematically in Fig. 1. For a more detailed description, see e.g. Huxley and Crompton (1974). A steady stream of electrons passes through a small circular aperture in the cathode and into a plane-parallel drift gap. Drift and diffusion subsequently bring the electrons to a collecting anode, which is divided into a central disk and an annular electrode—ideally stretching out to infinity. The currents I_i and I_o to the inner and outer parts of the anode are measured, and from their ratio one can find or estimate the value of D_T/μ.

Ideally, the entrance aperture should be vanishingly small—in practice not much larger than a mean free path—to allow the source to be approximated with a delta-function. Also, the electric field should be the same on the two sides of the entrance aperture, ensuring a 'properly conditioned' energy distribution for the electrons on entry into the drift gap. Finally, one would prefer both anode and cathode to be perfect absorbers, with electron reflection coefficient $\rho = 0$.

(2b) Current Ratio Formulae

We take the basic measured quantity to be the ratio between the current to the *outer* electrode and the total current,

$$R = I_o/(I_i + I_o)\,. \tag{1}$$

The length of the drift gap is h, the radius of the central disk is b, and the gap voltage $Eh = U$.

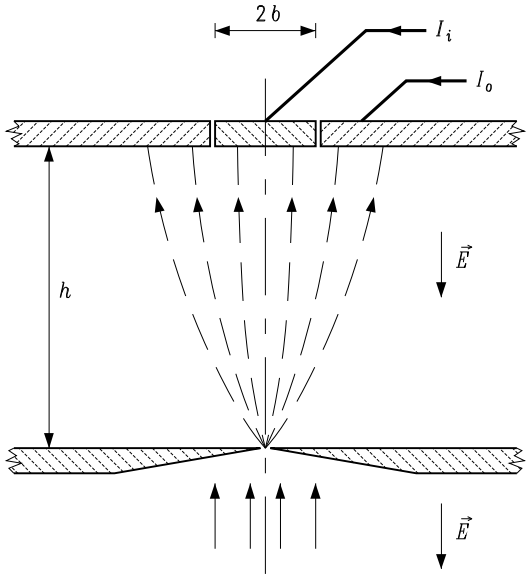

Fig. 1. The Townsend-Huxley experimental configuration, schematically.

An approximate expression for R is found by using Einstein's formula for the mean square radial displacement in a time t, replacing t by the mean drift time $h/v_{dr} = h/\mu E$, and assuming the current density J_z at the anode to be a Gaussian random process:

$$\langle r^2 \rangle_J \equiv \int r^2 J_z \mathrm{d}r^2 \Big/ \int J_z \mathrm{d}r^2 = 4D_T t\,, \tag{2}$$

$$t \to \overline{t} = h/\mu E\,, \tag{3}$$

$$J_z(h) \propto \exp(-r^2/\langle r^2 \rangle_J)\,. \tag{4}$$

This gives a ratio formula

$$R = \int_b^\infty J_z \mathrm{d}(r^2) \Big/ \int_0^\infty J_z \mathrm{d}(r^2) = \exp(-b^2/\langle r^2 \rangle_J)\,, \tag{5}$$

$$\langle r^2 \rangle_J = 4D_T h/\mu E = 4h^2(D_T/\mu)/U\,, \tag{6}$$

which we rewrite as

$$R = \exp[-\tfrac{1}{2}(b/h)^2/\delta_T]\,, \tag{7}$$

$$\delta_T = 2(D_T/\mu)/U\,. \tag{8}$$

In a typical experiment, b/h will be of order $0{\cdot}1$ and R in the range $0{\cdot}2$–$0{\cdot}8$ (Elford *et al.* 1992), and δ_T hence of order $0{\cdot}1$–1%.

More elaborate formulae for the ratio R have been derived by determining J_z from the diffusion equation,

$$\nabla \cdot \vec{J} = \nabla \cdot (n\vec{v}_{dr} - \vec{\vec{D}} \cdot \nabla n) = 0\,, \tag{9}$$

$$\vec{v}_{dr} = -v_{dr}\hat{E} \equiv v_{dr}\hat{z}\,, \tag{10}$$

$$\vec{\vec{D}} = D_L \hat{E}\hat{E} + D_T(\vec{\vec{1}} - \hat{E}\hat{E})\,. \tag{11}$$

Thus, assuming the density to be zero on the electrode surfaces (except in the entrance aperture), Lowke (1971) found an expression which may be written as

$$R = \delta_L^{-2}(t^{-3} + t^{-2} - \delta_L^{-1}t^{-1}) \exp(-t + \delta_L^{-1})\,, \tag{12}$$

$$\delta_L = 2(D_L/\mu)/U\,, \tag{13}$$

$$t = [1 + (D_L/D_T)(b/h)^2]^{\frac{1}{2}}/\delta_L\,. \tag{14}$$

Huxley (see Huxley and Crompton 1974) some years earlier had derived the expression (assuming isotropic diffusion)

$$R = t^{-1} \exp(-t + \delta_T^{-1})\,, \tag{15}$$

$$t = [1 + (b/h)^2]^{\frac{1}{2}}/\delta_T\,. \tag{16}$$

This derivation involved an error and it was therefore somewhat surprising that the Huxley formula was found to be, in most cases, an excellent approximation, yielding the same experimental D_T/μ values over a large range of pressures p, while the Lowke formula gives pressure-dependent values (Elford *et al.* 1992). Extrapolation of the values obtained from the two ratio formulae towards $p^{-1} \to 0$ gives, however, the same value within the experimental uncertainties.

(2c) Current Ratio Formulae and Transverse Position Moments

The various current ratio formulae (see Elford *et al.* 1992 for an extensive survey) apparently have very different forms. However, we know that they all in practice give quite similar results, and that the current distribution at the anode is rather close to the Gaussian of equation (4).

Slight and cylindrically symmetrical deviations from a Gaussian may be expressed in terms of a Laguerre polynomial series which, with the use of the correct variance, starts with the second order polynomial. A convenient approximate expression for the current density should thus be

$$J_z \propto \mathrm{e}^{-y}[1 + c_2 L_2(y) + \ldots]\,, \tag{17}$$

$$y = r^2/\langle r^2 \rangle_J\,. \tag{18}$$

Since higher order terms are damped out quickly by diffusion, one would expect a two-term expansion to be sufficiently accurate, giving rise to a current ratio formula

$$R = \mathrm{e}^{-y}[1 - c_2 y(2-y)]\,, \tag{19}$$

$$c_2 = \tfrac{1}{2}(\langle y^2\rangle - 2)\,. \tag{20}$$

In this approximation, R is determined by two parameters only, the variance $\langle r^2\rangle_J$ and the excess $\gamma_4 = 2(\langle r^4\rangle_J/\langle r^2\rangle_J^2 - 2) = 4c_2$. The Huxley and Lowke formulae give

$$\begin{aligned} &\text{Huxley}: \quad \langle r^2\rangle_J = \ 2h^2\delta_T; \qquad\qquad c_2 = \ \tfrac{1}{2}\delta_T\,. \\ &\text{Lowke}: \quad \langle r^2\rangle_J = \ 2h^2\delta_T(1-\delta_L); \quad c_2 = \ \tfrac{1}{2}\delta_L(1-\delta_L^2)/(1-\delta_L)^2\,. \end{aligned} \tag{21}$$

A numerical comparison between the exact Lowke and Huxley formulae and their respective two-parameter approximations reveals *no* noticeable differences in the experimentally interesting range of parameters. The most obvious difference between the Lowke and Huxley formulae is seen in the correction to the primitive expression for the variance (equation 5); the Huxley formula gives zero correction.

3. Kinetic Theory: Formulation of the Problem

(3a) Spatial Moments of the Boltzmann Equation

In order to make comparisons with the Lowke and Huxley expressions, we want to find the moments $\langle r^2\rangle_J$ and $\langle r^4\rangle_J$ of the current density at the anode, with electrons starting at the cathode in the position $(r = 0, z = 0)$, and without assuming hydrodynamic behaviour. It will, however, be more convenient to formulate the problem in Cartesian coordinates than in cylindrical coordinates, and calculate the moments $\langle x^2\rangle_J$ and $\langle x^4\rangle_J$ instead. Assuming cylindrical symmetry for the input distribution, we then have $\langle r^2\rangle_J = 2\langle x^2\rangle_J$ and $\langle r^4\rangle_J = 2(\langle x^4\rangle_J + \langle x^2\rangle_J^2)$.

The transverse moments of the current density are obtained from the stationary distribution function $f(\vec{r},\vec{v})$ as

$$\langle x^n\rangle_J/n! = \left\{\int (x^n/n!)v_z f(\vec{r},\vec{v})\mathrm{d}\vec{v}\mathrm{d}x\mathrm{d}y \Big/ \int v_z f(\vec{r},\vec{v})\mathrm{d}x\mathrm{d}y\right\}_{z=h} \tag{22}$$

$$\equiv \left\{\int v_z f^{[n]}(z,\vec{v})\mathrm{d}\vec{v} \Big/ \int v_z f^{[0]}(z,\vec{v})\mathrm{d}\vec{v}\right\}_{z=h}, \tag{23}$$

$$f^{[k]}(z,\vec{v}) = (1/k!)\int x^k f(\vec{r},\vec{v})\mathrm{d}x\mathrm{d}y\,. \tag{24}$$

Equations for the distribution moments $f^{[k]}$ are found by multiplication of the stationary Boltzmann equation

$$(\vec{v}\cdot\nabla + \vec{a}\cdot\nabla_{\vec{v}} + J)f(\vec{r},\vec{v}) = 0\,, \tag{25}$$

where $\vec{a} = -e\vec{E}/m$ is the acceleration of the electrons in the electrostatic field and J the collision operator, with $x^k/k!$ and subsequent integration over $\mathrm{d}x\mathrm{d}y$. This yields a hierarchy of equations

$$(v_z\partial_z + a\partial_{v_z} + J)f^{[k]}(z,\vec{v}) = v_x f^{[k-1]}(z,\vec{v})\,, \tag{26}$$

which can be solved for successively larger k-values, starting with the homogeneous $k = 0$ equation.

(3b) Spherical Harmonics Expansion

The collision operator J is spherically symmetric, and therefore has the spherical harmonics Y_{lm} as its directional eigenfunctions. To take advantage of this property, the distribution moments $f^{[k]}$ are conveniently expanded as

$$f^{[k]}(z,\vec{v}) = \Sigma_{l=0}^{l_{max}}\Sigma_{m=0}^{l} f_l^{[k,m]}(z,v)P_l^{[m]}(v_z/v)\cos(m\varphi)\,. \tag{27}$$

Inserting this expansion into the $f^{[k]}$-equation and projecting out the (l,m) component yields a system of equations

$$\begin{aligned}\frac{l+m+1}{2l+3}\left\{v(\partial_z + 2a\partial_{v^2}) + (l+2)\frac{a}{v}\right\}f_{l+1}^{[k,m]} \\ + \frac{l-m}{2l-1}\left\{v(\partial_z + 2a\partial_{v^2}) - (l-1)\frac{a}{v}\right\}f_{l-1}^{[k,m]} + J_l f_l^{[k,m]} = \overline{R}_l^{[k,m]}\,,\end{aligned} \tag{28}$$

$$\begin{aligned}\overline{R}_l^{[k,m]} = \tfrac{1}{2}v\left\{\frac{(l+m+1)(l+m+2)}{2l+3}f_{l+1}^{[k-1,m+1]} - \frac{(l-m-1)(l-m)}{2l-1}f_{l-1}^{[k-1,m+1]}\right\} \\ + \tfrac{1}{2}v\left\{\frac{1}{2l+1}f_{l-1}^{[k-1,m-1]} - \frac{1}{2l+3}f_{l+1}^{[k-1,m-1]}\right\}.\end{aligned} \tag{29}$$

In the present study, we restrict our attention to the quasi-Lorentz gas model, and the collision terms can then be written (see e.g. Kumar *et al.* 1980)

$$J_0 f_0^{[k,0]} = -2\frac{m}{m_0}v^{-1}\partial_{v^2}\left(v^3\nu_1\left[1 + 2\frac{k_B T}{m}\partial_{v^2}\right]f_0^{[k,0]}\right), \tag{30}$$

$$J_{l>0}f_l^{[k,m]} = \nu_l f_l^{[k,m]}\,, \tag{31}$$

$$\nu_l = n_0 v\sigma_l = n_0 v\int(1 - P_l(\cos\chi))\mathrm{d}\sigma\,, \tag{32}$$

where n_0 is the number density of the neutral gas, χ the c.m. deflection angle and $\mathrm{d}\sigma$ the differential cross section.

The moments $\langle x^2\rangle_J$ and $\langle x^4\rangle_J$ are found from the functions $f_1^{[2,0]}$ and $f_1^{[4,0]}$, respectively.

(3c) Boundary Conditions

In an actual experiment, some of the electrons impinging on the electrodes will be absorbed, and the rest will be reflected or re-emitted with some usually

unknown velocity distribution. In the present calculations, we will adopt a specular reflection model with an energy- and direction-independent reflection coefficient ρ, i.e. a part ρ of the electrons is assumed to be reflected elastically with velocity vector $(v_x, v_y, v_z) \rightarrow (v_x, v_y, -v_z)$. Our primary interest will be the case $\rho = 0$.

The input distribution is assumed given, and concentrated in the origin $(x = y = z = 0)$, i.e.

$$f_{in}^{[k]}(z = 0, \vec{v}) \overset{v_z \geq 0}{=} f_{in}(\vec{v})\, \delta_{0k}\,. \tag{33}$$

This gives as *exact* boundary conditions

$$f^{[k]}(z = 0, \vec{v}) \overset{v_z \geq 0}{=} \rho f^{[k]}(z = 0, -\vec{v}) + f_{in}(\vec{v})\, \delta_{0k}\,, \tag{34}$$

$$f^{[k]}(z = h, \vec{v}) \overset{v_z \leq 0}{=} \rho f^{[k]}(z = h, -\vec{v})\,. \tag{35}$$

In the ideal Townsend–Huxley experiment, we would have $f_{in}(\vec{v}) \propto f(h, \vec{v})_{v_z > 0}$.

In a truncated spherical harmonics expansion, these conditions can only be fulfilled approximately, as discussed in detail e.g. by Davison and Sykes (1957). The conceptually simplest would be to demand the conditions fulfilled in a discrete number of directions, corresponding to the order l_{max} of the spherical harmonics expansion, in such a way that the contributions from the first neglected component vanish—the so-called Mark condition. An alternative is to demand integrals over the boundary conditions to be fulfilled, e.g.

$$\int Y_{lm}(\hat{v})\{\text{Boundary conditions}\}\mathrm{d}\hat{v}\,, \tag{36}$$

using either only even or only odd l-values—so-called Marshak boundary conditions.

(3d) Length Scales and Admissible Approximations

There are a number of different length scales in electron transport problems, and if they differ sufficiently, the problems may be simplified by using different approximations on the different scales. Anisotropies relax typically on the scale of a mean free path for momentum transfer, while energies, assuming elastic collisions, relax on a scale of order $(m_0/m)^{\frac{1}{2}}$ larger.

The diffusion equation—with the x- and y-directions integrated out—has a general solution for the one-dimensional density $N(z)$ of the form

$$N(z) = a + b \exp[(v_{dr}/D_L)z]\,, \tag{37}$$

which indicates that the presence of the anode will have an influence over a hydrodynamic length scale of order D_L/v_{dr}. Assuming the approximate validity of the Nernst–Townsend relation, one will have $D_L/v_{dr} \sim k_B T_e/eE$, where T_e is the kinetic electron temperature. Finally, in thermal equilibrium the electron density should vary with the potential energy as $\exp(eU/k_B T) = \exp(-eEz/k_B T)$, with an associated thermodynamic length scale $k_B T/eE$, T being the *gas* temperature.

The relevant length scales are thus

$L_1 \sim 1/n_0\sigma_1$	Relaxation of anisotropies
$L_e \sim (m_0/m)^{\frac{1}{2}} L_1$	Relaxation of energies
$L_B \sim k_B T/eE$	Thermodynamic (Boltzmann factor)
$L_D \sim k_B T_e/eE$	Hydrodynamic (diffusion).

For sufficiently weak fields ($E \to 0$, $T_e \to T$), this yields three well separated length scales,

$$L_1 \ll L_e \ll L_B = L_D \,,$$

and three corresponding boundary layer regions; a thin region with large anisotropies and essentially constant energy distribution; a region of medium thickness with small anisotropies but varying energy distribution; and a hydrodynamic layer with nearly isotropic velocity distribution and nearly constant energy distribution.

For the strong field case ($T_e \gg T$ and $k_B T_e \sim eEL_e$), we find however only two well separated length scales,

$$L_1 \ll L_e \sim L_D \,,$$

while L_B shrinks towards zero. The merging of the energy relaxation and diffusion length scales means that there is no separate boundary region left where hydrodynamic theory gives an adequate description.

In the 'energy relaxation region', a two-term spherical harmonics expansion of the distribution function should be a sufficiently accurate description, while in the 'anisotropy relaxation region', a pure Lorentz gas description should be a good approximation.

4. Separation of Variables: Eigenfunction Expansion Methods

(4a) Velocity Moment Approach

The velocity moment method, in which the Boltzmann equation is transformed to a set of coupled velocity moment equations, has been very successfully used to find 'free space' electron transport properties, as outlined e.g. by Robson and Ness (1986). It would be calculationally very convenient if this method could be used also for the present type of problems.

The procedure consists in first choosing a suitable velocity space basis set $\{\varphi_j(\vec{v})\}$ and a complementary set of moment functions $\{\psi_i(\vec{v})\}$, inserting expansions

$$f^{[k]}(z, \vec{v}) = \Sigma_{j=1}^{N} Z_j^{[k]}(z)\varphi_j(\vec{v}) \tag{38}$$

in the kinetic equations, and forming equations for the expansion coefficients $Z_j^{[k]}(z)$ by multiplying with the moment functions and integrating over $\mathrm{d}\vec{v}$. This yields a system of equations of the form

$$B(\mathrm{d}/\mathrm{d}z)Z^{[k]} = MZ^{[k]} + D^{[k]}(z) \,, \tag{39}$$

where the matrix elements are

$$B_{ij} = \int v_z \psi_i(\vec{v}) \varphi_j(\vec{v}) \mathrm{d}\vec{v}\,, \tag{40}$$

$$M_{ij} = \int \psi_i(\vec{v}) \{a\partial_{v_z} + J\} \varphi_j(\vec{v}) \mathrm{d}\vec{v}\,, \tag{41}$$

$$D_i^{[k]} = \int v_x \psi_i(\vec{v}) f^{[k-1]}(z, \vec{v}) \mathrm{d}\vec{v}\,. \tag{42}$$

The general solution of the homogeneous equation ($k = 0$) may be written in form

$$Z^{[0]}(z) = \Sigma_{n=0}^{N} c_n^{[0]} \phi_n \exp(\lambda_n z)\,, \tag{43}$$

where (λ_n, ϕ_n) are the eigenvalues and eigenvectors of the generalised eigenproblem

$$B\phi = \lambda M \phi\,. \tag{44}$$

The solutions of the inhomogenous equations ($k > 0$) are obtained by adding convolution integrals to combinations of eigensolutions.

Numerical Method: Burnett Function Expansion. For mathematical convenience, we use as basis set the so-called Burnett functions (see e.g. Kumar *et al.* 1980),

$$\varphi_j(\vec{v}) \to \varphi_m^{(rl)}(\vec{v}/v_0)\,, \tag{45}$$

$$\varphi_m^{(rl)}(\vec{c}) \propto c^l Y_{lm}(\hat{c}) L_r^{(l+\frac{1}{2})}(c^2) \mathrm{e}^{-c^2}\,, \tag{46}$$

$$v_0 \sim \langle v^2 \rangle^{\frac{1}{2}}\,, \tag{47}$$

where $L_r^{(l+\frac{1}{2})}$ is an associated Laguerre polynomial, and as moment set the functions $\psi_j = \exp(c^2)\varphi_j$.

Grouping the matrix elements in blocks ordered after the l-indices, $\boldsymbol{M}$ becomes block tridiagonal, while in $\boldsymbol{B}$ only the blocks $(l, l \pm 1)$ are different from zero. For even l_{max} values, $\boldsymbol{B}$ is singular, and the eigenproblem has no solution. The basis set expansion thus has to be truncated at an odd value of l_{max}.

The eigenproblem was solved used the so-called QZ-algorithm (see e.g. Golub and van Loan 1983). Three scattering models were used, all assuming isotropic scattering ($\nu_{l>1} = \nu_1$); a constant collision frequency model, a constant cross section model, and an electron–helium model with cross sections σ_1 taken from Huxley and Crompton (1974). Even or odd Marshak type boundary conditions

$$\int \psi_m^{(rl)} \{\text{Boundary conditions}\} \mathrm{d}\vec{v}$$

were then applied to find the expansion coefficients c_n. Unphysical solutions are avoided by using proper 'half-space expansions' (see e.g. Davison and Sykes 1957), i.e. only eigensolutions with $\lambda_n \leq 0$ are used at the cathode and correspondingly only those with $\lambda_n \geq 0$ at the anode.

Results—and Problems. The method described above worked reasonably well in the case of weak electric fields, i.e. when the electron mean energy was less than about 20% above the thermal energy. The eigenvalues λ fell into three different groups; the steady state value $\lambda = 0 \cdot 0$ and the thermodynamic value $\lambda = eE/k_BT$; values of order $1/L_1 \sim 1/n_0\sigma_1$; and values of order $1/L_e \sim (m/m_0)^{\frac{1}{2}}/L_1$. In a two-term expansion ($l_{max} = 1$), the group $\lambda \sim 1/L_1$ disappeared, as expected.

A problem arose with the constant cross section model beyond the two-term approximation. The expansions in this case failed to converge, essentially because the large $\lambda \sim 1/L_1$ eigenvalues became degenerate—reflecting the lack of variation of the length scale with energy. The problem was overcome by using a modified two-term expansion, where 'one-energy group' results (see e.g. Williams 1971) were used to relate the $f_{l>1}$ to f_1 at the electrode. Comparison with Monte Carlo simulations—which we have routinely run for testing—showed this to introduce negligible error. The trick can be used also for other scattering models, and for most practical purposes one can thus reduce the problems to 'two-term calculations with one-energy-group anisotropy corrections'.

When the electric field was increased, the method ceased to give useful results in the *anode* region, i.e. when $\lambda_n > 0$. The first indication of trouble was that the positive eigenvalues changed from being real to occur in complex conjugate pairs. This was accompanied by basis size dependent oscillations in the calculated density and mean energy profiles. Further increase of the field gave 'number out of range' type results.

In the cathode region, no such problems occurred. However, since the anode problem could not be solved, it also became impossible to determine the proper input distribution.

To check the current ratio formulae for the Townsend–Huxley experiment, we calculated the variance $\langle r^2 \rangle_J$ at the anode, using the constant mean free time model and the helium model, at fields low enough to avoid complex eigenvalues. The hydrodynamic electron temperature T_e could then typically be increased to order 10% above the gas temperature. The relative corrections to the variance were found to agree with the prediction of the Lowke formula (equation 12) within $1 \cdot 2\%$ for the helium model*, and within from $0 \cdot 2\%$ at vanishing field to 12% at the highest field for the constant mean free time model.

The Lowke formula thus gives an excellent approximation to the correction to the variance $\langle x^2 \rangle_J$ at weak fields ($\langle x^4 \rangle_J$ was not calculated).

(4b) Constant Mean Free Time Model: Exact Two-term Eigensolutions

The velocity moment method just described has as its key ingredient the solution of a generalised eigenproblem related to the operator $v_z^{-1}(a\partial_{v_z} + J)$. When the method converges, the calculated eigenvalues should be expected to approach the exact eigenvalues of this operator, and the eigenfunctions to approach the exact eigenfunctions. The problems associated with the method—the lack of convergence for the positive eigenvalue part at intermediate and strong fields—may henceforth reflect problems connected with the forms of the exact spectra and

* Already at these low E/N values, the difference between longitudinal and transverse diffusion is substantial, and it is necessary to use the quantity δ_L and not δ_T in the correction formula to get this degree of agreement.

eigenfunctions. The problems are related only to the energy relaxation modes, and can therefore be studied in a two-term approximation.

It turns out that for the constant collision frequency model, the eigenfunctions and the spectrum can be found analytically, as will be outlined below.

The Eigenproblem and Its Structure. The equations to be solved are the direct eigenequation

$$(a\partial_{v_z} + J)\varphi = -\lambda v_z \varphi \,, \tag{48}$$

$$\varphi = \varphi_0(v) + (v_z/v)\varphi_1(v) \,, \tag{49}$$

and the adjoint equation

$$(-a\partial_{v_z} + \tilde{J})\psi = -\lambda v_z \psi \,, \tag{50}$$

$$\psi = \psi_0(v) + (v_z/v)\psi_1(v) \,, \tag{51}$$

where $\tilde{J}$ is the adjoint collision operator, defined by the relation $\int \psi(J\varphi)\mathrm{d}\vec{v} = \int \varphi(\tilde{J}\psi)\mathrm{d}\vec{v}$.

The function sets $\boldsymbol{\varphi}$ and $\boldsymbol{\psi}$ are biorthogonal, with orthogonality relation

$$(\lambda_i - \lambda_j)\int v_z \varphi_i \psi_j \mathrm{d}\vec{v} = 0 \,. \tag{52}$$

In an expansion of some function $f(\vec{v})$ in eigenfunctions φ_i, the expansion coefficients can be found using $\int \mathrm{d}\vec{v} v_z \psi_i \ldots$ as a projection operator—if the expansion exists.

Letting $\partial_z \to \lambda$ in the two-term kinetic equations, and assuming $\nu_1(v) \to \nu =$ const., we obtain

$$\lambda v\varphi_1 + a\left(\frac{2}{v} + \frac{\mathrm{d}}{\mathrm{d}v}\right)\varphi_1 - 3\frac{m}{m_0}\nu v^{-2}\frac{\mathrm{d}}{\mathrm{d}v}(v^3\varphi_0) - 3\nu\frac{k_BT}{m_0}v^{-2}\frac{\mathrm{d}}{\mathrm{d}v}\left(v^2\frac{\mathrm{d}}{\mathrm{d}v}\varphi_0\right) = 0 \,, \tag{53}$$

$$\lambda v\psi_1 - a\left(\frac{2}{v} + \frac{\mathrm{d}}{\mathrm{d}v}\right)\psi_1 + 3\frac{m}{m_0}\nu v^{-2}\frac{\mathrm{d}}{\mathrm{d}v}(v^3\psi_0) - 3\nu\frac{k_BT}{m_0}v^{-2}\frac{\mathrm{d}}{\mathrm{d}v}\left(v^2\frac{\mathrm{d}}{\mathrm{d}v}\psi_0\right) = 0 \,, \tag{54}$$

$$\lambda v\varphi_0 + a\frac{\mathrm{d}}{\mathrm{d}v}\varphi_0 + \nu\varphi_1 = 0 \,, \tag{55}$$

$$\lambda v\psi_0 - a\frac{\mathrm{d}}{\mathrm{d}v}\psi_0 + \nu\psi_1 = 0 \,. \tag{56}$$

Eliminating φ_1 and ψ_1, and introducing new quantities

$$v_W^2 = 3k_BT/m + (m_0/m)(a/\nu)^2 \equiv v_T^2 + v_E^2 \,, \qquad x = \tfrac{3}{2}v^2/v_W^2 \,,$$

$$\Lambda^2 = (m_0/m)(\lambda/\nu)^2 v_W^2 \,, \qquad \epsilon = v_E/v_W \,, \tag{57}$$

these equations are transformed to

$$x\mathrm{d}^2\varphi_0/\mathrm{d}x^2 + [\tfrac{3}{2} + (1+\tfrac{2}{3}\epsilon\Lambda)x]\mathrm{d}\varphi_0/\mathrm{d}x + [\tfrac{3}{2} + \epsilon\Lambda/2 + (\Lambda^2/9)x]\varphi_0 = 0\,, \quad (58)$$

$$x\mathrm{d}^2\psi_0/\mathrm{d}x^2 + [\tfrac{3}{2} - (1+\tfrac{2}{3}\epsilon\Lambda)x]\mathrm{d}\psi_0/\mathrm{d}x + [-\epsilon\Lambda/2 + (\Lambda^2/9)x]\psi_0 = 0\,. \quad (59)$$

It is easily seen from this that φ_0 and ψ_0 are related by

$$\psi_0 \propto \varphi_0 \exp[(1+\tfrac{2}{3}\epsilon\Lambda)x]\,. \quad (60)$$

The equations can be transformed to a standard form by methods as described e.g. by Zwillinger (1989). We first insert for φ_0 an expression

$$\varphi_0(x) = g(x)\mathrm{e}^{-\alpha x} \quad (61)$$

to get an equation for $g(x)$

$$x\mathrm{d}^2g/\mathrm{d}x^2 + [\tfrac{3}{2} + (1+\tfrac{2}{3}\epsilon\Lambda - 2\alpha)x]\mathrm{d}g/\mathrm{d}x$$

$$+[\tfrac{3}{2}(1-\alpha) + \epsilon\Lambda/2 + \{\alpha^2 - \alpha(1+\tfrac{2}{3}\epsilon\Lambda) + (\Lambda^2/9)\}x]g = 0\,. \quad (62)$$

By choosing α to fulfill the condition

$$\alpha^2 - \alpha(1+\tfrac{2}{3}\epsilon\Lambda) + \Lambda^2/9 = 0 \quad (63)$$

and introducing a new variable

$$z = (2\alpha - 1 - \tfrac{2}{3}\epsilon\Lambda)x\,, \quad (64)$$

this is transformed to a Laguerre equation

$$z\mathrm{d}^2g/\mathrm{d}z^2 + [\tfrac{3}{2} - z]\mathrm{d}g/\mathrm{d}z + ng = 0\,, \quad (65)$$

$$n = (\tfrac{3}{4})\{-1 + 1/(2\alpha - 1 - \tfrac{2}{3}\epsilon\Lambda)\} \quad (= 0, 1, 2\ldots)\,, \quad (66)$$

with solution $g \propto L_n^{(1/2)}(z)$. From this we find the eigenvalues and eigenfunctions to be

$$\Lambda_n^{(\pm)} = \tfrac{3}{2}\frac{\epsilon}{1-\epsilon^2}\left(1 \pm \left[1 + \frac{1-\epsilon^2}{\epsilon^2}\frac{n(n+\frac{3}{2})}{(n+\frac{3}{4})^2}\right]^{\frac{1}{2}}\right), \quad (67)$$

$$\varphi_0^{(n)} = L_n^{(1/2)}\left(\frac{3}{3+4n}x\right)\exp\left[-\left(\frac{3+2n}{3+4n} + \epsilon\Lambda_n/3\right)x\right], \quad (68)$$

$$x\varphi_1^{(n)} = -(6m/m_0)^{\frac{1}{2}}[\Lambda x\varphi_0/3 + \epsilon x\mathrm{d}\varphi_0/\mathrm{d}x]\,. \quad (69)$$

The eigenfunctions $\varphi_0^{(n)}$ are quite similar in appearance to the so-called Pagani eigenfunctions found for the corresponding Rayleigh gas problem (see e.g. Burscha and Titulaer 1982).

Eigenfunctions, Spectra and Halfspace Completeness. At weak fields, $\epsilon \to 0$, the 'forwards and backwards propagating eigenfunctions' (corresponding to negative and positive eigenvalues, respectively) transform into each other on the operation $z \to -z$, with the eigenvalues Λ and the factor in the exponent of the eigenfunction $\mathrm{E}(\varphi)$ approaching

$$\Lambda_n^{\pm} \overset{\epsilon \to 0}{\to} \pm \tfrac{3}{2}[n(n+\tfrac{3}{2})/(n+\tfrac{3}{4})^2]^{\frac{1}{2}} = \pm[0, 1\cdot3535, 1\cdot4431, \ldots, 1\cdot50)\,, \tag{70}$$

$$\mathrm{E}(\varphi^{(n)}) \overset{\epsilon \to 0}{\to} -\frac{3+2n}{3+4n}x = -[1, 0\cdot7143, 0\cdot6364, \ldots, 0\cdot50)x\,, \tag{71}$$

with $x \to mv^2/2k_BT$.

The exponents are all of the order of the thermal Maxwellian values, and any essentially thermal distribution $f_0 + (v_z/v)f_1(v)$ ought to be expandable in either of the two sets of eigenfunctions, thus making it possible to satisfy the two-term boundary conditions.

At strong fields, $\epsilon \to 1$, the situation is drastically different. The 'cathode eigensolutions' have eigenvalues and exponents corresponding to the energy relaxation length scale L_e and mean steady state energies $mv_W^2/2$,

$$\Lambda_n^{-} \overset{\epsilon \to 1}{\to} -\tfrac{3}{4}n(n+\tfrac{3}{2})/(n+\tfrac{3}{4})^2 = -[0, 0\cdot6122, 0\cdot6942, \ldots, 0\cdot75)\,, \tag{72}$$

$$\mathrm{E}(\varphi_-^{(n)}) \overset{\epsilon \to 1}{\to} -\frac{(3+2n)(3+6n)}{(3+4n)^2}x = -[1, 0\cdot9184, 0\cdot8678, \ldots, 0\cdot75)x\,, \tag{73}$$

while the 'anode eigensolutions' are essentially thermal,

$$\Lambda_n^{+} \overset{\epsilon \to 1}{\to} 3v_E^2/v_T^2 \to \infty\,, \tag{74}$$

$$\lambda_n^{+} \overset{\epsilon \to 1}{\to} (m/m_0)(\nu^2/a)\Lambda_n^{+} \to eE/k_BT\,, \tag{75}$$

$$\mathrm{E}(\varphi_+^{(n)}) \overset{\epsilon \to 1}{\to} -\left(\frac{3+2n}{3+4n} + \Lambda_n^{+}/3\right)x \to -mv^2/2k_BT\,. \tag{76}$$

To satisfy the anode boundary condition—assuming for the moment a perfectly absorbing electrode—one has to subtract the negative halfspace part of the 'hydrodynamic' $\lambda = 0$ mode φ_0^- from the distribution function, i.e. one has to perform the expansion

$$\exp(-x) \overset{v_z/v<0}{=} \Sigma c_n^{+} \varphi_+^{(n)}\,, \tag{77}$$

to get the full anode space solution

$$f(z, \vec{v}) \propto \mathrm{e}^{-x} - \Sigma c_n^{+} \varphi_+^{(n)} \mathrm{e}^{-\lambda_n^{+}(h-z)}\,. \tag{78}$$

It is immediately clear that a function $\exp(-x)$ cannot be expanded in polynomials around another exponential $\exp(-x/x_0)$, when $x_0 \sim T/T_e \ll 1$. Thus, the 'anode

eigensolutions' do not form a complete set in the relevant function space at strong fields.

(4c) Summary of Findings

At weak fields, i.e. when the free space steady state kinetic energy of the electrons is not more then 10–20% above the thermal energy, the velocity moment approach works nicely. Approximate eigenvalues and eigenfunctions are found, Marshak type boundary conditions are easily fulfilled, and the position moment $\langle r^2 \rangle_J (z = h)$ can be calculated accurately—the calculations giving results in close agreement with the prediction of Lowke's current ratio formula.

By using simple one-energy-group results for correction, one can truncate the spherical harmonics expansion of the distribution at $\mathrm{l}_{max} = 1$, without significant error.

For the constant collision frequency model, exact eigenfunctions have been found. An attempt to use these in further calculations was however not very successful—the expansions of the anode and cathode distribution functions in exact eigenfunctions converge extremely slowly. This was as expected, however, from results for the rather similar quasi-Rayleigh gas problem (Burscha and Titulaer 1982; Naqvi *et al.* 1984).

The velocity moment method becomes unsuitable at stronger fields, for the *anode* problem. A physical explanation of this failure can be given as follows. The exact eigenfunctions, as well as the approximate eigenfunctions found in the velocity moment approach, reflect how a 'free space system' by itself can generate distribution modes $\varphi(z, \vec{v})$. There are two sources of energy available, the electric field and the thermal motions of the gas molecules. The electric field can furnish energy only to electrons drifting in the direction of the electric force, i.e. in the positive z-direction—and therefore can only contribute to the mean energy for the $\lambda \leq 0$ eigenfunctions. Modes propagating and decaying in the direction *against* the field can only aquire energy from the thermal motions—and the $\lambda > 0$ eigenfunctions hence all have mean energies of order the thermal energy, and a spatial behaviour approximately given by the Boltzmann factor $\exp(eEz/k_B T)$.

To satisfy the anode boundary condition, the negative halfspace part of the distribution function must be expanded in backwards propagating eigenfunctions. However, when the electron kinetic temperature T_e is not close to the gas temperature T, this expansion diverges—and divergence in fact occurs already at $(T_e/T - 1) \sim 0 \cdot 25$.

The difficulties in modelling the anode region at strong fields arise from a physically unsound separation of variables $f \rightarrow \Sigma Z(z) W(v^2) Y_{lm}(\hat{v})$. This is most easily seen by considering a cold gas model, where the electrons will never *gain* energy in a collision: The anode problem can be viewed as a problem of describing the 'missing electrons'—those that would have travelled backwards from the anode if it were not there. Between collisions, the 'missing electrons' will move on characteristics $(mv^2/2 - eEz) = \text{constant}$, while the collisions will take them from one of these characteristics to another one with lower total energy. They can thus *not* move backwards from the anode without losing kinetic energy. The separation of variables used in the foregoing does, however, implicitly assume that this is possible.

The anode problem—and preferrably the whole slab problem—should, in view of this, be reformulated in coordinates which reflect the coupling between kinetic and potential energy. The anode and cathode boundaries would then, however, no longer coincide with any coordinate axes, and this would introduce some new complications. These should however not be as fatal as those resulting from the present approach.

5. The Cold Gas Model: A Finite Difference Approach

The correction terms in the current ratio formula (equation 19) are of order $(D/\mu)/U$, and will only be of importance when the mean electron energy $m\langle v^2\rangle/2 \sim eD/\mu$ is not small compared to eU. In a real experiment, one will always have $eU \gg k_BT$, and the correction terms are hence only of practical importance at strong fields, i.e. when $m\langle v^2\rangle \gg k_BT$. To investigate this case, we will model the Townsend–Huxley experiment numerically in the cold gas limit $k_BT \to 0$, using a finite difference approach. The thermal motions may be included afterwards as perturbation terms, if felt necessary.

(5a) Kinetic Equations and Boundary Conditions

We want to find the second and the fourth transverse position moment at the anode. In the spherical harmonics representation of the $f^{[k]}$s, these are given by

$$(\tfrac{1}{2})\langle x^2\rangle_J = \int v f_1^{[2]} \mathrm{d}\vec{v} \Big/ \int v f_1^{[0]} \mathrm{d}\vec{v}\,, \tag{79}$$

$$(\tfrac{1}{4}!)\langle x^4\rangle_J = \int v f_1^{[4]} \mathrm{d}\vec{v} \Big/ \int v f_1^{[0]} \mathrm{d}\vec{v}\,. \tag{80}$$

In a two-term approximation, one will only have to solve equations for a few $f_l^{[k]}$ to find these moments—and two of these equations are trivial (see equations 28 and 29);

$$f^{[0]} = f_0^{[0]} + (v_z/v) f_1^{[0]}\,, \tag{81}$$

$$f^{[1]} = (v_x/v) f_1^{[1]} = (v_x/v)(v/\nu) f_0^{[0]}\,, \tag{82}$$

$$f^{[2]} = f_0^{[2]} + (v_z/v) f_1^{[2]}\,, \tag{83}$$

$$f^{[3]} = (v_x/v) f_1^{[3]} = (v_x/v)(v/\nu) f_0^{[2]}\,, \tag{84}$$

$$f^{[4]} = f_0^{[4]} + (v_z/v) f_1^{[4]}\,. \tag{85}$$

Further, the $f_1^{[k]}$ for even k are obtained directly from the corresponding f_0;

$$f_1^{[k]} = -(v/\nu)(\partial_z + 2a\partial_{v^2}) f_0^{[k]} \quad (k = 0, 2, 4)\,, \tag{86}$$

and can be eliminated from the kinetic equations, to give

$$(\partial_z + 2a\partial_{v^2})(v^3/\nu)(\partial_z + 2a\partial_{v^2})f_0^{[k]}$$
$$+6\frac{m}{m_0}\partial_{v^2}\left(v^3\nu\left[1+2\frac{k_BT}{m}\partial_{v^2}\right]f_0^{[k]}\right) = \begin{cases}(v^3/\nu)f_0^{[k-2]} & k\ =\ 2{,}4\\ 0 & k\ =\ 0\end{cases}. \quad (87)$$

We use Mark boundary conditions, i.e. we demand equations (34) and (35) to be fulfilled at the zeros of $P_2(v_z/v)$, that is for $v_z/v = \pm 1/\sqrt{3}$. This will result in an error of order $0{\cdot}2$ mean free paths in the so-called Milne extrapolation length (see e.g. Williams 1971), which is irrelevant in the present context. The boundary conditions can then be written, after eliminating the f_1,

$$\left\{v(\partial_z + 2a\partial_{v^2}) + \frac{1-\rho}{1+\rho}\nu\sqrt{3}\right\}f_0^{[k]} = 0 \qquad \text{anode} \quad (88)$$

$$\left\{v(\partial_z + 2a\partial_{v^2}) - \frac{1-\rho}{1+\rho}\nu\sqrt{3}\right\}f_0^{[k]} = -\frac{1}{1+\rho}\nu\sqrt{3}\,f_{in}\,\delta_{0k} \quad \text{cathode.} \quad (89)$$

To make the equations more amenable for numerical computation, we introduce a suitable hydrodynamic length scale L_D and corresponding dimensionless quantities:

Hydrodynamic length scale : $L_D = D_T/v_{dr}$

Microscopic length unit : $\lambda_0 = (3m/m_0)^{\frac{1}{2}}L_D$

Cross section unit : $\sigma_0 = 1/n_0\lambda_0$

Reduced cross section : $s = \sigma/\sigma_0$

Reduced temperature : $\Theta = (k_BT/m)/(aL_D)$
$= (k_BT)/(eD_T/\mu)$

Reduced length : $\zeta = z/L_D = (3m/m_0)^{\frac{1}{2}}z/\lambda_0$

Reduced energy : $\eta = (3m/m_0)^{\frac{1}{2}}v^2/2a\lambda_0$
$= (mv^2/2)/(eD_T/\mu)$

to get the kinetic equations in the form

$$(\partial_\zeta + \partial_\eta)(\eta/s)(\partial_\zeta + \partial_\eta)f_0^{[k]} + 2\partial_\eta(\eta^2 s f_0^{[k]})$$
$$= -2\Theta\partial_\eta(\eta^2\partial_\eta f_0^{[k]}) + L_D^2\,(\eta/s)\,f_0^{[k-2]}\,. \quad (90)$$

For the cold gas case, $\Theta = 0$, these are parabolic equations, which are readily changed into canonical form by the coordinate transformations

$$p = \eta + \zeta\,, \qquad \eta = (p+q)/2\,,$$
$$q = \eta - \zeta\,, \qquad \zeta = (p-q)/2\,, \quad (91)$$

which give

$$\partial_q(\eta^2 s f_0^{[k]}) = \partial_p(\eta^2 s f_0^{[k]}) + 2\partial_p[(\eta/s)\partial_p] f_0^{[k]} - \tfrac{1}{2} L_D^2\,(\eta/s) f_0^{[k-2]} + \mathcal{O}(\Theta)\,. \tag{92}$$

We note that the characteristics $q =$ constant are curves of constant total energy—and that the transformation to the canonical form thus has forced on us coordinates taking proper account of the coupling between kinetic and potential energy.

The transformed anode and cathode boundary conditions are

$$\frac{1-\rho}{1+\rho} f_0^{[k]} + (2/s)(m/m_0)^{\frac{1}{2}} \partial_p f_0^{[k]} = 0 \qquad \text{anode} \tag{93}$$

$$\frac{1-\rho}{1+\rho} f_0^{[k]} - (2/s)(m/m_0)^{\frac{1}{2}} \partial_p f_0^{[k]} = \frac{1}{1+\rho} f_{in} \delta_{0k} \quad \text{cathode}\,. \tag{94}$$

(5b) Solution Method

The kinetic equations (92) were solved numerically—with $\Theta = 0$—using the Crank–Nicholson finite difference scheme (see e.g. Press *et al.* 1989), using collision models of type $\nu \propto v^\gamma$. The coordinate system and the direction of integration are illustrated in Fig. 2. The coordinate system is similar to the one used by Sugawara *et al.* (1992) in a study of the steady state Townsend experiment. The integration would start at ($\zeta = 0$, $\eta = \eta_{max}$) and proceed from one constant total energy characteristic to the next by the solution of a tridiagonal matrix equation, to end up at ($\zeta = \zeta_h$, $\eta = 0$).

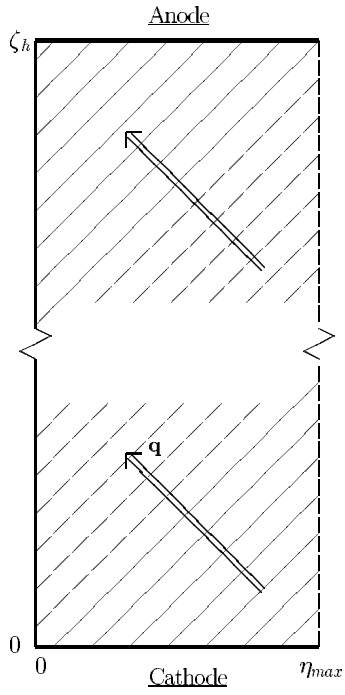

Fig. 2. Coordinate system used for integrating the cold gas kinetic equations.

Two extra boundary conditions had to be added, at $\eta \to 0$ and at $\eta = \eta_{max}$, the chosen cut-off value. These boundaries are in a sense non-physical. No electron will ever come totally to rest ($\eta = 0$), and η_{max} should be chosen large enough that only a negligible portion of the electrons would ever reach the corresponding kinetic energy.

For the η_{max} boundary, a perfectly absorbing boundary condition was used (equation 93 with $\rho = 0$). This gave smoother solutions at large η-values than e.g. to force the distribution—or its derivative—to zero at this boundary.

In the $\eta \to 0$ limit, it has been argued that a correct condition to use would be a demand that the distribution be continuous at $\vec{v} = 0$ (see e.g. Segur *et al.* 1983). In the two-term approximation, this implies that $f_1 \overset{v\to 0}{\longrightarrow} = 0$. However, in the cold gas case this condition can only be justified if $\sigma_1(v) \overset{v\to 0}{\longrightarrow} \sigma_0 = \text{constant}$, i.e. for $\gamma = 1$ in our calculations, and it also turned out to give numerically unstable results for other γ-values. We chose instead to use a weaker 'free boundary condition',

$$\partial_p^2 f_0^{[k]} \overset{v\to 0}{\longrightarrow} 0\,,$$

also taking care not to place grid points on the $\eta = 0$ axis—and this worked well.

To start the integration from the cathode, the anode distribution was needed, and was therefore calculated first. This calculation only necessitated considering the upper left triangle in Fig. 2 ($\eta \le \eta_{max}$, $\zeta \ge \zeta_h - \eta_{max}$), as the anode boundary is without influence outside this region.

At the cathode boundary, it was necessary to modify the difference scheme to connect properly the high and low η regions on the cathode surface. In the 'cathode triangle' of Fig. 2, a (p, η) finite difference scheme—with inferior stability properties—was therefore used instead of the (p, q) scheme.

The calculations were started using a small gap length ζ_h, and the length was subsequently increased until the numerically calculated values of $\langle x^2 \rangle_J$ and the excess γ_4 showed the expected asymptotic behaviour $\langle x^2 \rangle_J \propto \zeta_h$ and $\gamma_4 \propto 1/\zeta_h$.

(5c) Numerical Results

Calculations were performed with collision frequencies $\nu \propto v^\gamma$, and $\gamma \in [-0{\cdot}5, 2{\cdot}0]$. For $\gamma < -0{\cdot}5$, our numerical scheme—which used constant step sizes $(\Delta p, \Delta q)$—became unstable. To investigate the possible influence of the surface conditions, two different reflection coefficients were used, $\rho = 0$ (our ideal model experiment), and $\rho = 0{\cdot}9$. Further, to see how a neglect of the variation of the energy distribution in the electrode layers would affect the results, we performed calculations not only with the anode distribution as input, but also using the free space steady state distribution.

The main results were the values of the relative correction to the variance of the anode current distribution (see equation 21),

$$\begin{aligned}\delta_2 &= (\langle r^2 \rangle_J/2 - h^2\,\delta_T)/\delta_T^2 \\ &= (\langle r^2 \rangle_J/2 - 2hD_T/v_{dr})/(2D_T/v_{dr})^2\,, \end{aligned} \tag{95}$$

and the reduced excess

$$\delta_4 = \tfrac{1}{2}\gamma_4\,\zeta_h, \qquad \text{where} \qquad \zeta_h = h/(2D_T/v_{dr})\,. \tag{96}$$

Fig. 3 shows the variation of δ_2 with the gap length ζ_h, for the constant mean free path ($\gamma = 1$) and the constant mean free time ($\gamma = 0$) models, and two different input distributions. Perfect absorption ($\rho = 0$) was assumed. The differences between the 'S' curves and the 'A' curves reflect the energy relaxation processes in the cathode region. The 'S' curves reach asymptotic values in a distance of order one hydrodynamic relaxation length. In the 'A' case, the cathode distribution has a larger mean energy than the steady state and, therefore the rate of diffusion is initially larger than for the 'S' case. For 'soft' interactions ($\gamma < 0$), fast electrons collide less often than slow ones, and the cooling regions in these cases therefore stretch considerably further out in the gap than suggested by the hydrodynamic length scale.

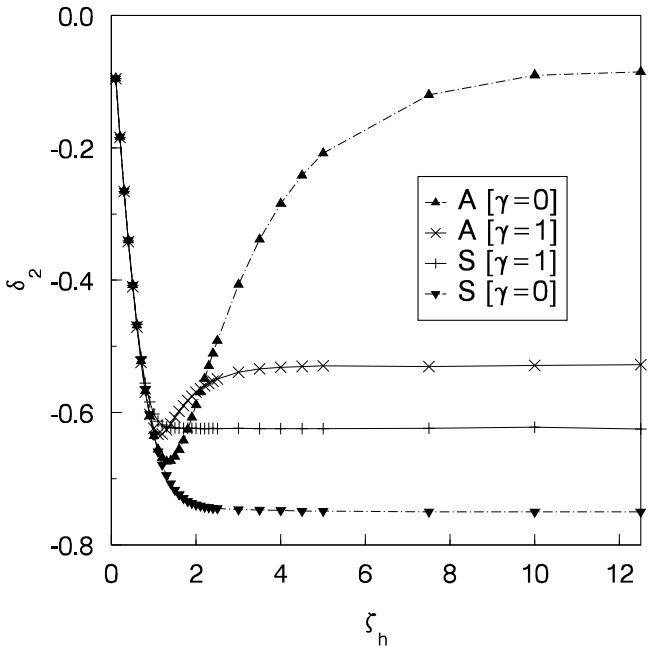

Fig. 3. Relative correction δ_2 (see equation 95) to the variance of the anode current distribution, as a function of the reduced gap length ζ_h, for the constant mean free path ($\gamma = 1$) and the constant mean free time ($\gamma = 0$) models: A, 'anode' input distribution; S, 'steady state' input distribution.

Calculations for other γ-values showed an increasingly longer 'cooling length' with decreasing γ, reflecting the very long high energy tails of the corresponding velocity distributions and the reduction of collision probability with increasing energy.

In an actual diffusion experiment, the reduced gap length ζ_h will always be large, and only values of δ_2 and δ_4 in the limit $\zeta_h \to \infty$ are therefore of practical importance. Fig. 4 and Fig. 5 show these limiting values as functions of γ. Also shown are the values predicted by Lowke's current ratio formula (equation 12).

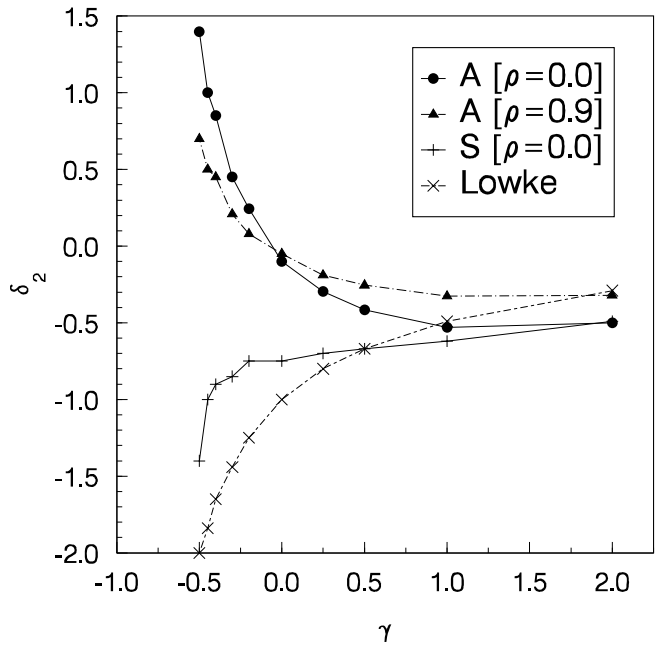

Fig. 4. Asymptotic ($\zeta_h \to \infty$) value of the relative correction δ_2 (equation 95) to the variance of the anode current distribution, as a function of the interaction parameter γ ($\nu \propto v^\gamma$): A, 'anode' input distribution; S, 'steady state' input distribution.

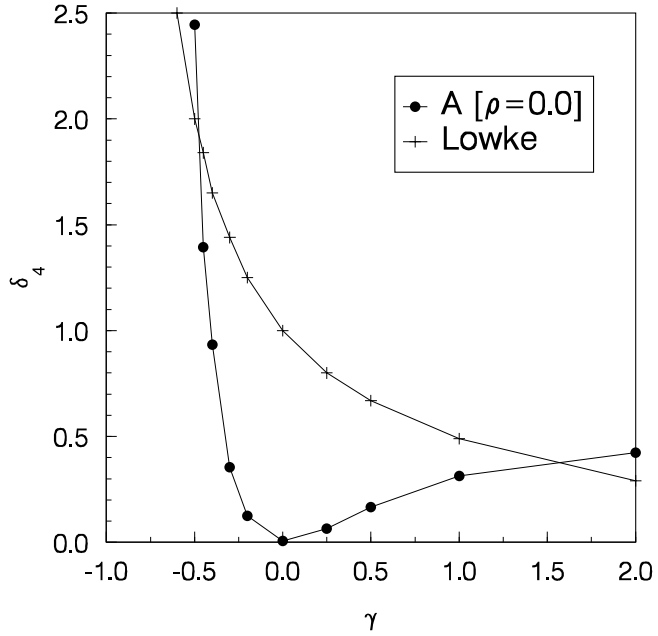

Fig. 5. Asymptotic ($\zeta_h \to \infty$) value of the reduced excess δ_4 (equation 96) for the ideal Townsend–Huxley experiment, as a function of the interaction parameter γ ($\nu \propto v^\gamma$).

The δ_2 values in Fig. 4 were obtained with 'anode distribution input' and reflection coefficients $0{\cdot}0$ and $0{\cdot}9$, and with 'steady state input' and reflection coefficient $0{\cdot}0$. The Lowke formula approximates the steady state input results reasonably well, but when the more realistic 'anode input' is used it even gives the wrong sign for the correction when $\gamma < 0$. Huxley's current ratio formula predicts $\delta_2 = 0{\cdot}0$, which is a better overall approximation. The value of the reflection coefficient is obviously not of great importance.

The limiting δ_4 values were, within a few percent, independent of both input distribution and reflection coefficient. In Fig. 5 we therefore show only one set of results—for anode distribution input and $\rho = 0$. There is no striking similarity between the calculated curve and the one obtained from the Lowke formula—or from the Huxley formula, which predicts $\delta_4 = 1$. Neither of those formulae show a minimum of $\delta_4 \approx 0$ at $\gamma \approx 0$.

6. Conclusions

The Townsend–Huxley transverse diffusion experiment has been modelled by formulating the associated kinetic theory problem in the form of transverse position moments of the distribution function, and solving the kinetic equations by two complementary methods. At near-thermal electron energies, a velocity moment based eigenfunction expansion method was used, and at high electron energies—the 'cold gas limit'—a finite difference scheme in 'skewed coordinates'. As a by-product of the studies, we have also found exact eigenfunctions for the 'slab problem', for the constant collision frequency model in the two-term approximation.

The eigenfunction expansion methods do not take implicitly into account the coupling between kinetic and potential energy. As a direct result of this, they cannot be used to model the *anode* region except at very weak fields. This finding should apply also to other 'external field slab problems'. However, it seems as if a coordinate transformation might possibly lead to a way of bypassing this shortcoming.

An analysis of the form of the various current ratio formulae existing in the literature revealed that they all—for practical purposes—can be fully characterised by only the second and the fourth transverse position moment of the current density at the anode.

The difference between Huxley's formula (see Huxley and Crompton 1974) and Lowke's (1971) formula is to be found mainly in the value they predict for the second moment. Huxley's formula just gives the simple estimate

$$\langle r^2 \rangle_J = 4 D_T h / v_{dr} \,,$$

without any correction at all, while Lowke's formula adds to this a multiplicative factor

$$1 - 2(D_L/\mu)/U \,,$$

where U is the gap voltage. These two formulae give essentially the same expression for the fourth order distortion from a Gaussian current density profile, apart from a factor D_L/D_T.

The velocity moment calculations showed the Lowke formula to give an excellent estimate of the magnitude of the end effects at electron energies close to thermal. This is as expected from a consideration of the hydrodynamic length scale, since $L_D \sim D/v_{dr}$ is large compared to the kinetic energy relaxation length scale. However, at weak fields the boundary effects are not of practical importance in the Townsend–Huxley experiment.

The strong field calculations showed that the corrections to the simple expression for $\langle r^2 \rangle_J$ depend strongly on the velocity distribution of the electrons on entry into the diffusion gap—and on how the distribution subsequently relaxes towards the free space steady state distribution. The form of the input distribution, and the energy relaxation, are not—and cannot be—taken into account in hydrodynamic theory. The corrections are most important for 'soft' interaction models $\gamma < 0$. For these models, the Lowke formula gives corrections of the wrong sign. On the other hand, the Huxley formula implies no corrections, and is better for that reason.

The value of the electron reflection coefficient of the electrodes is of only minor importance for the correction factors. This observation may seem to be in some contrast with the findings of Braglia and Lowke (1979). However, their calculations were based on an extremely 'hard' interaction model, where the corrections are not of significance anyhow.

For practical purposes it seems as if the simple ratio formula given by equations (5) and (6),

$$R = \exp\{-\tfrac{1}{4}(b/h)^2 U/(D_T/\mu)\}\,,$$

will be as good as any, and this simplifies the analysis of the experiments. When end effects *are* of importance, 'differencing' seems to be the only certain way of proceeding to obtain correct D_T/μ values.

Acknowledgments

The authors are grateful to Dr M. T. Elford for advice and discussions from the start of this work, and to him and Dr K. Kumar for reading and commenting on the manuscript. A major part of the work was performed with the support of a Post. Doc. grant (to JPE) from The Norwegian Research Council.

References

Beals, R., and Protopopescu, V. (1983). *J. Stat. Phys.* **32,** 565.
Braglia, G. L. (1982). *Phys. Rev.* A **25,** 1214.
Braglia, G. L. and Lowke, J. J. (1979). *J. Phys.* D **12**, 1831.
Burscha, M. A., and Titulaer, U. M. (1982). *Physica* A **112**, 315.
Cole, R. G., Keyes, T., and Protopopescu, V. (1984). *J. Chem. Phys.* **81**, 2771.
Davison, B., and Sykes, J. B. (1957). 'Neutron Transport Theory' (Oxford University Press).
Elford, M. T., Brennan, M. J., and Ness, K. F. (1992). *Aust. Phys.* **45**, 671.
England, J. P., and Skullerud, H. R. (1991). Joint Symposium on Electron and Ion Swarms and Low Energy Electron Scattering (Bond University, Queensland, Australia).
England, J. P., and Skullerud, H. R. (1993). 8th International Swarm Seminar (University of Trondheim, Norway).
Golub, G. H., and van Loan, C. F. (1983). 'Matrix Computations' (Johns Hopkins: Baltimore).
Huxley, L. G., and Crompton, R. W. (1974). 'The Diffusion and Drift of Electrons in Gases' (John Wiley: New York).

Kumar, K., Skullerud, H. R., and Robson, R. E. (1980). *Aust. J. Phys.* **33**, 343.
Lowke, J. J. (1971). Proc. 10th Int. Conf. on Phenomena in Ionised Gases (Oxford).
Lowke, J. J., Parker, J. H., and Hall, C. A. (1977). *Phys. Rev.* A **15**, 1237.
Naqvi, K. R., Waldenstrøm, S., and Mork, K. J. (1984). *Arkiv for Det Fysiske Seminar i Trondheim no. 14*.
Press, W. H., Flannery, B. P., Teukolsky, S. A., and Vetterling, W. T. (1989). 'Numerical Recipes in Pascal' (Cambridge University Press).
Robson, R. E. (1981). *Aust. J. Phys.* **34**, 223.
Robson, R. E. (1995). *Aust. J. Phys.* **48**, 347.
Robson, R. E., and Ness, K. (1986). *Phys. Rev.* A **33**, 2068.
Segur, P., Bordage, M-C., Balaguer, J-P., and Yousfi, M. (1983). *J. Comput. Phys.* **50**, 116.
Sugawara, H., Sakai, Y., and Tagashira, H. (1992). *J. Phys.* D **25**, 1483.
Williams, M. M. R. (1971). 'Mathematical Methods in Particle Transport Theory' (Butterworths: London).
Zwillinger, D. (1989). 'Handbook of Differential Equations' (Academic: New York).

Manuscript received 3 July, accepted 1 October 1996